ORIGINAL RESEARCH

# Quantitative Fiber Tracking of the Optic Radiation Is Correlated with Visual-Evoked Potential Amplitude in Preterm Infants

H.C. Glass
J.I. Berman
A.M. Norcia
E.E. Rogers
R.G. Henry
C. Hou
A.J. Barkovich
W.V. Good

**BACKGROUND AND PURPOSE:** Children born preterm are at risk for adverse outcome, including visual impairment. We examined the relationship between neonatal DTI and sVEP in children born preterm to determine whether visual outcomes are related to early measurements of brain microstructure.

**MATERIALS AND METHODS:** Subjects were born at <34 weeks gestation and imaged before term-equivalent age. DTI fiber tracking was used to delineate the optic radiations and measure tract-specific average FA, $D_{av}$, and parallel and transverse diffusivity. Visual-evoked response amplitudes were measured as a function of spatial frequency, contrast, and vernier offset size with sVEP at 6–20 months after birth. The association between DTI and sVEP was assessed by using the Spearman correlation coefficient and linear regression for repeated measures.

**RESULTS:** Nine children with 15 scans were included. The peak response amplitudes for spatial frequency sweeps were associated with increasing FA and decreasing $D_{av}$ and transverse diffusivity ($P \leq .006$) but not with parallel diffusivity ($P = 1$). There was only modest association with the swept contrast condition and no detectable association with the vernier offset sweeps.

**CONCLUSIONS:** Microstructure of the optic radiations measured shortly after birth is associated with quantitatively measured responses elicited by moderate-to-high contrast spatiotemporal gratings in infancy. These findings are in keeping with studies showing a relationship between brain microstructure and function. While the clinical impact is not known, quantitative neuroimaging of white matter may ultimately be important for predicting outcome in preterm neonates.

**ABBREVIATIONS:** BSID = Bayley Scales of Infant Development; cpd = cycles per degree; $D_{av}$ = mean apparent diffusion coefficient; DTI = diffusion tensor imaging; FA = fractional anisotropy; IVH = intraventricular hemorrhage; MRI = MR imaging; NIH = National Institutes of Health; PVHI = periventricular hemorrhagic infarct; sVEP = swept parameter visual-evoked potential; WMI = white matter injury

According to the Centers for Disease Control and Prevention, the rate of preterm delivery has increased steadily and now accounts for 12.5% of births in the United States.[1] Recent advances in neonatology have led to improved survival rates in preterm infants, and the therapeutic focus has shifted toward early detection and treatment of neurodevelopmental disabilities, including motor, cognitive, and visual deficits. Children born preterm are at risk for visual impairment due to cerebral visual impairment, which is caused by damage to the geniculocalcarine pathways and is related to the severity of white matter injury.[2-4] Children with cerebral visual impairment often have comorbid neurologic impairments, including mental retardation, cerebral palsy, and hearing loss.[5]

In preterm infants, the periventricular white matter is particularly susceptible to injury. White matter contains important subcortical pathways, including the corticospinal tracts and optic radiations.[6] Severe injury to the periventricular white matter can be identified by transfontanel sonography; however, this technique may miss more subtle injuries that are evident only by MR imaging.[7,8] Recent studies have shown that very low-birth-weight infants without sonographic evidence of intracranial injury are spared from major disruptions in visual system function.[9] However, little is known about the relationship between more subtle differences in brain development and subclinical visual impairment or their relationship to minor cognitive impairment.

DTI is a noninvasive MR imaging tool, which can be used to assess in vivo brain maturation in preterm neonates (reviewed in Mukherjee and McKinstry[10] and Huppi and Dubois[11]). This imaging technique makes use of the random motion of water molecules to assess tissue microstructure and detect changes in brain maturation. Diffusion anisotropy depends on the degree of myelination; orientation, number, and compactness of axons; and the presence of other cells such as glia and makes DTI a good tool for studying white matter changes through development and with injury. We recently

Received December 21, 2009; accepted after revision February 28, 2010.

From the Departments of Pediatrics (H.C.G., E.E.R.), Neurology (H.C.G.), Radiology and Biomedical Imaging (J.I.B., R.G.H., A.J.B.), and Ophthalmology (W.V.G.), University of California, San Francisco, San Francisco, California; and Smith-Kettlewell Eye Research Institute (A.M.N., C.H., W.V.G.), San Francisco, California.

H.C. Glass and J.I. Berman contributed equally to this work.

This work was supported by NIH/NCRR/OD UCSF-CTSI grant KL2 RR024130 (H.C.G.) and by grants from the National Eye Institute (EY00384 WVG and AMN) and the National Institute of Neurological Disorders and Stroke (R01 NS046432).

The views expressed herein are solely the responsibility of the authors and do not necessarily represent the official views of the NIH.

Paper previously presented as a poster at: Annual Meeting of the Child Neurology Society, October 14–17, 2009; Louisville, Kentucky.

Please address correspondence to Hannah C. Glass, MD, Department of Neurology, University of California, San Francisco, Box 0663, 521 Parnassus Ave, C-215, San Francisco, CA 94143-0663; e-mail: Hannah.Glass@ucsf.edu



DOI 10.3174/ajnr.A2110

showed that DTI can be used for fiber tracking of the unmyelinated optic radiations in premature neonates and that there is a relationship between white matter microstructure and visual performance in this population.[12]

sVEP is a technique that allows quantitative electrophysiologic assessment of the cortical response to different types of visual stimuli in nonverbal subjects. In this study, we performed 3 assays of spatiotemporal vision: spatial frequency tuning (voltage as a function of the spatial scale of the stimulus), a measurement of the contrast response function (voltage as a function of contrast at low spatial frequency), and a measure of response amplitude as a function of vernier offset size. The sVEP has been successfully used for quantifying visual function in typically-developing infants.[9,13-16]

The purpose of this study was to evaluate the relationship between microstructure of the optic radiations and a functional measure of vision to determine whether disruption of that microstructure might be predictive of functional outcome. We confirm that brain microstructure as assessed by DTI in the early neonatal period is robustly associated with response amplitudes generated by moderate-to-high-contrast low spatial frequency targets in infancy. This quantitative study uses sVEP to measure vision, and adds to previous qualitative (behavioral) studies that suggested an association between white matter integrity and visual function.[12,17]

## Materials and Methods

The study subjects were infants of <34 weeks gestation at birth who were admitted to the intensive care unit at the University of California, San Francisco Medical Center and enrolled into a cohort study examining MR imaging predictors of neurodevelopmental outcome. Exclusion criteria were clinical evidence of a congenital malformation, congenital infection, syndromic diagnosis, or retinopathy of prematurity of more than stage II disease. The Committee for Human Research approved the study protocol, and children were studied only after informed parental consent.

From April 2006 to June 2007, 9 infants were enrolled, scanned with MR imaging in the neonatal period, and studied with the sVEP protocol in infancy as described below.

### *Clinical Data Collection*

Trained neonatal research nurses prospectively extracted clinical data from maternal and infant medical records. Gestational age was calculated on the basis of the last menstrual period or early sonography (<24 weeks). In cases in which the difference between the 2 methods exceeded 7 days, the sonography date was used.

### *MR Imaging*

Serial MR imaging was performed according to protocol, initially when the infant was stable for transport (mean postmenstrual age, 33.1 weeks) and again at term-equivalent age or before hospital transfer or discharge (mean postmenstrual age, 37.5 weeks). MR images were acquired by using a 1.5T Signa scanner (GE Healthcare, Milwaukee, Wisconsin) and a specialized high-sensitivity neonatal head coil built into the MR imaging–compatible incubator.[18] If necessary, infants were sedated according to institution guidelines. Anatomic imaging sequences included axial spin-echo T2-weighted and coronal volumetric 3D spoiled gradient-echo T1-weighted images, acquired as previously reported.[19] Diffusion-weighted images were obtained with a 4.8-minute single-shot echo-planar sequence with TR/TE = 7 seconds/100 ms, 256 × 128 matrix, 1.4 × 1.4 mm in-plane resolution, 3-mm-thick contiguous sections, 360 × 180 mm FOV, 167-kHz bandwidth, and 3 acquisition averages. Diffusion-weighting gradients were applied in 6 noncolinear directions at $b = 600$ s/mm$^2$ in addition to a $b = 0$ s/mm$^2$ volume. A 2D 10th-order nonlinear registration algorithm was used to correct for motion[20,21] by using the $b = 0$ s/mm$^2$ volume as a reference for the diffusion-weighted volumes. Smoothed diffusion-weighted images were produced by averaging a 3 × 3 voxel in-plane neighborhood, and associated diffusion metrics were calculated for each voxel from the smoothed and unsmoothed diffusion-weighted images.[22] The smoothed diffusion metric maps were used for region-of-interest placement and DTI fiber tracking. To reduce partial volume averaging, we used the unsmoothed diffusion metric maps for tract-specific measurements. DTI fiber tracking and tract-specific quantification were performed by using software written with Interactive Data Language (ITT Visual Solutions, Boulder, Colorado) as previously described.[12]

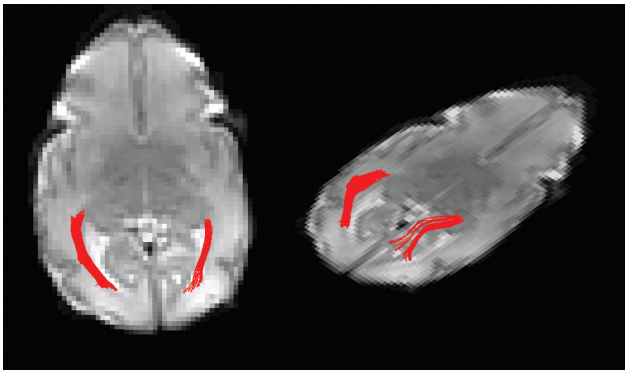

**Fig 1.** Two views of the left and right optic radiations from a single subject born at 28 4/7 weeks gestation and imaged at 33 3/7 weeks gestation.

Starting regions of interest for fiber tracking were placed in the white matter adjacent to the lateral geniculate nucleus. A single experienced scientist (J.I.B.) drew the starting and target regions of interest. The regions were drawn larger than and surrounding the tract of interest. Thus, the borders of the region of interest rarely passed through the optic radiation and did not limit the border of the 3D region defined by fiber tracking. The 3D tract was defined by the fiber tracking algorithm by using large start and target regions of interest so that operator-dependent effects were minimized. Target regions were drawn in the white matter adjacent to the primary visual cortex. Fiber tracks originating in the starting region and passing through the target region were retained as the delineated optic radiation as shown in Fig 1. Fiber tracks were terminated if they entered a voxel with FA < 0.05 or turned more than 50° between 2 adjacent voxels. The FA threshold is above the noise floor but low enough to successfully perform fiber tracking in unmyelinated tracts with low anisotropy. Measurements of diffusion metrics including FA, eigenvalues ($\lambda_1$, $\lambda_2$, $\lambda_3$), and $D_{av}$ within the optic radiation were made on the basis of the voxels containing DTI fiber tracks. "Transverse diffusivity" represents diffusion orthogonal to axonal bundles and is the average of $\lambda_2$ and $\lambda_3$. Measurements were taken from the entire optic radiation, and left- and right-sided optic radiation measurements within a patient were averaged.

Two neuroradiologists who were blinded to the subject's clinical condition evaluated the MR images to identify white matter injury, intraventricular hemorrhage, and periventricular hemorrhagic infarct as previously described.[23]

### *sVEP Parameter Technique*

The sVEP technique has been described in detail previously.[13,24] The electroencephalogram signal intensity was amplified by using a Model 12 amplifier (Grass Technologies, West Warwick, Rhode Island) (filter settings: 1–100 Hz at −6 dB) at a gain of 20,000. Active electrodes were placed at Oz, O1, and O2 with a reference electrode at Cz and a ground at Pz, according to the International 10–20 System.[25] Electrode impedance was ≤10 kΩ. Data acquisition and stimulus presentation were controlled by using an in-house software system.[24] Stimuli were presented on a high-bandwidth monochrome monitor (MR2000HB-MED; Richardson Electronics, Sykesville, Maryland) at a screen resolution of 1600 × 1200 pixels and a 60-Hz vertical refresh rate.

A small toy was dangled 0–2 cm from the screen to direct the infant's attention toward the monitor during the trials, each of which lasted 10 seconds. Viewing was binocular from 100 cm while the infant was seated in a parent's lap. Spatial frequency tuning was measured at 80% contrast over a sweep linear range from 2 to 16 cpd. Contrast response functions were measured by presenting a phase-reversing 2-cpd sine wave grating, which was swept logarithmically from 0.5% to 20% contrast over the 10-second trial. Vernier offset response functions were measured by using a 2-cpd grating carrier also shown at 80% contrast, into which vernier displacements were periodically introduced and removed. The sweep range for vernier displacements was 8–0.5 arc minutes (equal log spacing). Grating phase reversals and vernier offset alternation were all modulated at 3.76 Hz. The swept parameter presentations were repeated 4–8 times to improve the signal intensity-to–noise ratio by averaging out the uncorrelated background activity.

### *sVEP Analysis*

The group average evoked-response functions were each monotonically increasing functions of stimulus intensity for each sweep type.[9] We, therefore, used the peak voltage attained at the midline occipital lead for each sweep type in each subject for comparison with the DTI parameters.

### *Neurodevelopmental Follow-Up*

All infants enrolled in the study were evaluated periodically in the High-Risk Infant Follow-Up Clinic at our institution. A developmental psychologist who was blinded to the neonatal course examined the children by using the BSID (3rd edition).[26] A developmental pediatrician or a neurologist performed a structured neurologic examination.

### *Statistical Analysis*

Statistical analysis was performed by using STATA 10 software (StataCorp, College Station, Texas). Differences between clinical predictors were assessed by using the 2-tailed Student *t* test for continuous variables and the $\chi^2$ or Fisher exact test for categoric variables. Association between DTI parameters ($D_{av}$, FA, and transverse and parallel diffusivity) and visual outcomes was assessed by using Spearman correlation coefficients and generalized estimating equations for repeated measures.[27]

## Results

Nine infants completed the study protocol. MR images were of high-enough quality to complete DTI fiber tracking in 15 scans (Table). The mean gestational age at birth was 28.9 ± 2 weeks, mean birth weight was 1115 ± 362 g, and 56% of the subjects were male. None of the infants had strabismus or nystagmus. On the conventional MR images, 2 neonates had white matter injury and 1 neonate had intraventricular hemorrhage plus periventricular hemorrhagic infarct.

**General characteristics of 9 preterm newborns evaluated using MR imaging and sVEP**

| General Characteristics | Postmenstrual Age at MRI (weeks) | Conventional MRI Results | Corrected Age at sVEP (mo) | Outcome |
|---|---|---|---|---|
| 29 Weeks<br>Male<br>Singleton<br>913 g | 31<br>40 1/7 | Normal | 8.1 | Normal exam<br>BSID III 85<br>(28 mo) |
| 26 3/7 Weeks<br>Female<br>Singleton<br>900 g | 34<br>39 6/7 | Normal | 11.9 | Normal exam<br>BSID III 115<br>(29 mo) |
| 28 2/7 Weeks<br>Male<br>Singleton<br>1190 g | 29 1/7<br>32 6/7 | IVH with PVHI | 9 | Mild diplegia<br>BSID III 100<br>(30 mo) |
| 31 1/7 Weeks<br>Twin<br>875 g | 33 3/7 | Normal | 18.3 | Normal exam<br>BSID III 90<br>(37 mo) |
| 32 3/7 Weeks<br>Twin<br>1770 g | 33 4/7 | Moderate WMI | 10.5 | Normal exam<br>BSID III 125<br>(31 mo) |
| 32 3/7 Weeks<br>Twin<br>1840 g | 34 1/7<br>39 4/7 | Moderate WMI | 10.5 | Normal exam<br>BSID III 135<br>(31 mo) |
| 28 4/7 Weeks<br>Singleton<br>1115 g | 33 3/7<br>36 3/7 | Normal | 13.4 | Normal exam<br>BSID III 130<br>(30 mo) |
| 28 6/7 Weeks<br>Twin<br>1040 g | 34 5/7 | Normal | 9 | Normal exam<br>BSID III 135<br>(14 mo) |
| 28 6/7 Weeks<br>Twin<br>1150 g | 34 2/7<br>36 2/7 | Normal | 9 | Normal exam<br>BSID III 120<br>(14 mo) |

Age at follow-up examination was at a median of 30 months (range, 14–37 months). The cognitive subscale of the BSID (3rd edition) was within the normal range for all children (median, 120; range, 85–135). The neurologic examination findings were normal in all children, with the exception of the child with the intraventricular hemorrhage plus periventricular hemorrhagic infarct, who had mild spastic diplegia.

### *sVEPs*

Infants were examined by using sVEP at a median corrected gestational age of 10.5 months (range, 8–18 months). There was no apparent association between gestational age at birth (*P* values all > .8), sex (*P* values all > .5), or corrected age at the time of the evoked-potential examination (*P* values all > .2) and the sVEP peak amplitude responses for each of the 3 visual paradigms. There was also no measurable association between MR imaging findings of white matter injury (*P* values all > .9) or hemorrhage (*P* values all > .1) and each of the sVEP responses.

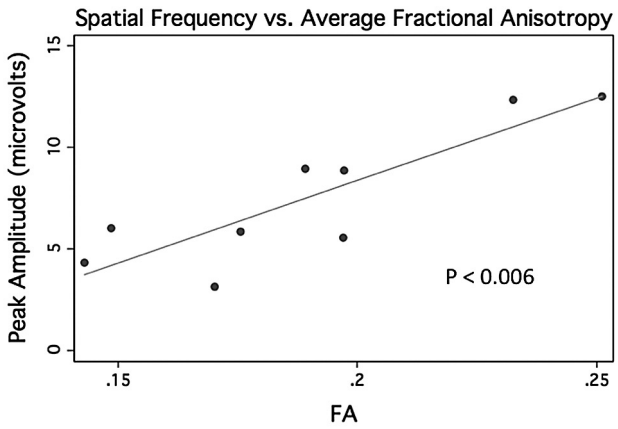


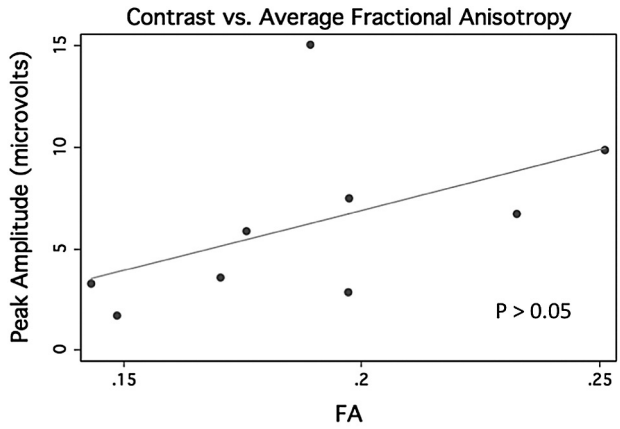


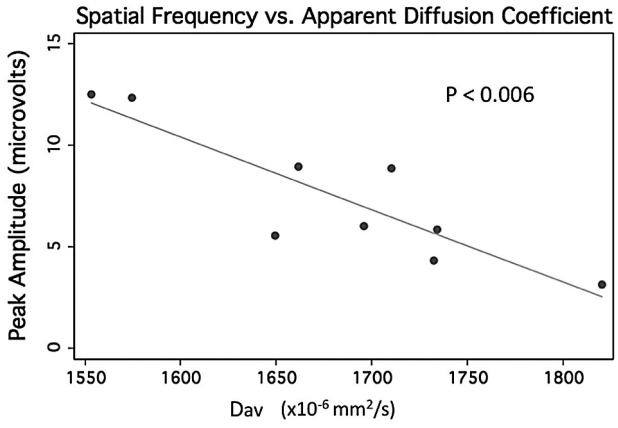


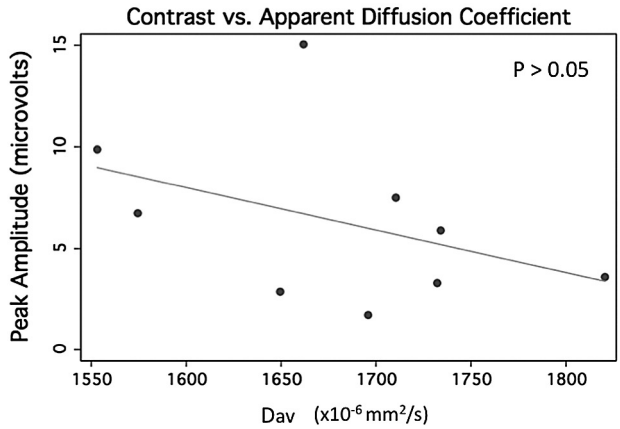


**Fig 2.** Peak amplitude from spatial frequency sweep trials versus average FA (top) and versus apparent diffusion coefficient derived from the early MR imaging in 9 preterm neonates.

**Fig 3.** Peak amplitude from contrast sweep trials versus average FA (top) and versus apparent diffusion coefficient derived from the early MR imaging in 9 preterm neonates.

### *DTI Data*

The peak response amplitudes for spatial frequency sweeps were robustly associated with the increasing FA, and decreasing $D_{av}$ (Spearman $\rho$, 0.7–0.8; with $P < .003$ and $P < .006$ after adjusting for repeated measures in the regression analysis) (Fig 2). The peak response amplitudes for spatial frequency sweeps were associated with the average transverse diffusivity (average of $\lambda_2$ and $\lambda_3$; Spearman $\rho$, 0.8; $P = .0003$) but not the parallel diffusivity ($\lambda_1$; Spearman $\rho$, 0.4; $P = .1$).

The modest association between peak response amplitudes for the contrast response function and FA and $D_{av}$ was not significant by using the Spearman correlation (Spearman $\rho$, 0.4; $P = .2$) (Fig 3). A similar trend was seen with the transverse diffusivity (average of $\lambda_2$ and $\lambda_3$; Spearman $\rho$, 0.4; $P = .2$) more closely associated than the parallel diffusivity ($\lambda_1$; Spearman $\rho$, 0.04; $P = .9$). The peak response amplitudes for vernier offset response function were also not associated with the diffusion parameters (Spearman $\rho$, 0.1–0.3; $P > .2$ for all measures including the analysis accounting for repeated measures) (Fig 4).

### *Multivariable Analysis*

There was no change in these associations after adjusting for the gestational age at the time of MR imaging in the regression model.

### *Sensitivity Analysis*

There was no change in the associations when the analysis was restricted to those children with normal findings on conventional imaging, though the *P* values were less robust for the spatial frequency sweeps.

## Discussion

This study shows that in children born preterm, the microstructure of the optic radiations (as measured with diffusion MR imaging before term-equivalent age) is associated with quantitative measures of visual function assessed in infancy. $D_{av}$ and FA were robustly associated with the spatial-frequency paradigm, indicating an overall relationship between microstructure integrity and the visual response. The findings are in keeping with the fact that both peak sVEP amplitudes and DTI parameters reflect the attenuation and organization of axonal membranes and myelination.[28] However, the sVEP responses were associated with transverse but not parallel diffusion. Because parallel diffusivity is theorized to correlate with axonal density, and transverse diffusion with the degree of myelination, these results indicate that processes associated with myelination may play a primary role in the correlation between DTI measures and sVEP.[29]

The diffusion parameters were robustly correlated with the peak response amplitudes for spatial-frequency sweeps, whereas they had only a modest association with contrast

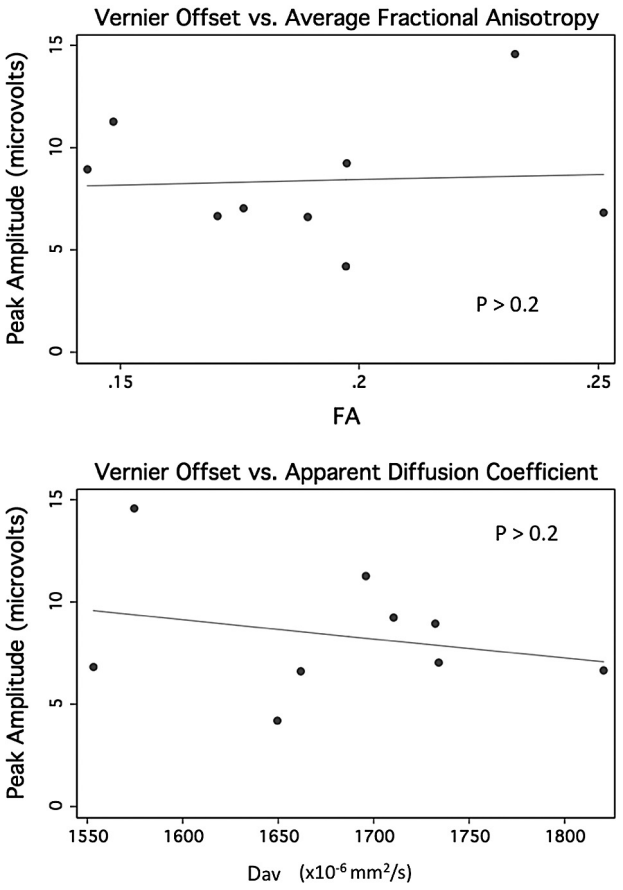


**Fig 4.** Peak amplitude from vernier offset sweep trials versus average FA (top) and versus apparent diffusion coefficient derived from the early MR imaging in 9 preterm neonates.

sweeps and no apparent association with vernier acuity. The difference in the relationship between DTI parameters and the visual assays may reflect differences in the physiologic processes that limit performance on the tasks or the fiber tracking technique. When comparing the spatial frequency and contrast sweep paradigms, the gratings were similar in spatiotemporal frequency but were higher contrast in the spatial frequency sweep. For these trials, the largest amplitudes were obtained during the low spatial frequency stimuli. The response to higher contrast in the spatial frequency sweep may have been individually more reliable than the midlevel contrasts attained at the end of the contrast sweeps, and this may have resulted in a more robust correlation with the DTI parameters.

There are 2, possibly related, reasons why responses to the vernier offset target did not correlate with the DTI parameters. The first is that the peak amplitudes in the vernier sweep trial occur for a stimulus that contains a wide range of spatial frequencies. It is possible that preferential losses occur predominantly for low rather than medium or high spatial frequencies and that the vernier response is specifically spared. Alternatively, it is possible that this stimulus relies on a different subset of optic radiation fibers and that these fibers may have been differentially excluded from the measurements we made. The greater relationship with transverse diffusivity compared with parallel diffusivity may reflect the early processes related to myelination (so-called "premyelination") of the preterm brain. Before term-equivalent age, the optic tracts are undergoing the physiologic changes that set the stage for myelination, which include changes to ion channels and the extension of oligodendroglial processes to the axon.[30,31]

The sVEP measurements and DTI fiber tracking probe the function and structure of the optic radiation. However, DTI fiber tracking cannot fully delineate the entire optic radiation because of technique limitations. DTI fiber tracking may fail to delineate the optic radiation where the tract turns sharply or crosses other white matter tracts. In addition, fiber tracking delineates the white matter course of the optic radiation and does not directly reflect structural or functional abnormalities within the cortex. These constraints may limit the measurement region to the core of the optic radiation and may not include parts of the tract important for individual sVEP responses. The use of a 1.5T (rather than 3T) scanner for the DTI and only 6 directions of diffusion encoding may result in a lower sensitivity to microstructural changes; however, with the use of a specially-designed high-sensitivity neonatal head coil, DTI at 1.5T can accurately quantify white matter tracts in preterm neonates.[12,32-34]

Another potential limitation is the wide age range (5–18 months) at the time of the outcome measure. We do not expect that this impacted our results, given that the response pattern for spatial frequency and contrast sensitivity have matured by this time.[24,35] Furthermore, there was no association between age and the visual parameters in this cohort. Finally, this study is limited by the small size of the cohort, which reduces our ability to firmly conclude that some visual functions are spared while others are lost and may also account for the lack of association seen with the vernier responses.

These quantitative results are consistent with studies showing that DTI is associated with functional measures of vision. Our group recently studied 36 preterm neonates from a similar cohort and showed that DTI fiber tracking was associated with a simple bedside ophthalmologic examination of visual fixation and alignment.[12] Bassi et al[17] similarly showed that DTI was associated with a standardized examination that tests visual attention for distance, color, and stripe discrimination. Dubois et al[36] examined 15 healthy term-born infants to show that there is a quantitative relationship between the microstructural maturation of the optic radiations, as measured by using DTI parameters, and a quantitative measure of visual development, the P1 latency of the visual-evoked potential. Ours is the first study to show a relationship between DTI measured early in the perinatal period and visual function measured up to 1 1/2 years later. This relationship between early measures of microstructure and later functional outcome at a time when myelination is more mature suggests that early imaging of the microstructure may be associated with long-term differences in development.

There is increasing evidence that diffusion MR imaging parameters are associated with functional measures in children at risk for brain injury.[37-41] However, the predictive value of these measures is not yet known. Additional studies relating diffusion metrics and outcome will be important to better understand how these measures may help with prognostication of visual function and neurodevelopment in children born preterm. Early identification of children at risk for visual impairment could lead to improved developmental outcomes

through early referral for visual services. Furthermore, DTI measures may be a good biomarker for studies that examine risk factors for brain injury, as well as trials of novel neuroprotective agents.


### *Acknowledgments*

We thank Ms Amy J. Markowitz for her assistance with manuscript preparation and David Glidden, PhD, and John Boscardin, PhD, for their assistance with the statistical analysis.


## References


1. Hoyert DL, Mathews TJ, Menacker F, et al. **Annual summary of vital statistics: 2004.** *Pediatrics* 2006;117:168–83
2. Cioni G, Fazzi B, Coluccini M, et al. **Cerebral visual impairment in preterm infants with periventricular leukomalacia**. *Pediatr Neurol* 1997;17:331–38
3. Lanzi G, Fazzi E, Uggetti C, et al. **Cerebral visual impairment in periventricular leukomalacia**. *Neuropediatrics* 1998;29:145–50
4. Uggetti C, Egitto MG, Fazzi E, et al. **Cerebral visual impairment in periventricular leukomalacia: MR correlation**. *AJNR Am J Neuroradiol* 1996;17:979–85
5. Matsuba CA, Jan JE. **Long-term outcome of children with cortical visual impairment**. *Dev Med Child Neurol* 2006;48:508–12
6. Volpe JJ. *Neurology of the Newborn*. Philadelphia: Saunders; 2008
7. Inder TE, Anderson NJ, Spencer C, et al. **White matter injury in the premature infant: a comparison between serial cranial sonographic and MR findings at term**. *AJNR Am J Neuroradiol* 2003;24:805–09
8. Miller SP, Cozzio CC, Goldstein RB, et al. **Comparing the diagnosis of white matter injury in premature newborns with serial MR imaging and transfontanel ultrasonography findings**. *AJNR Am J Neuroradiol* 2003;24:1661–69
9. Mirabella G, Kjaer PK, Norcia AM, et al. **Visual development in very low birth weight infants**. *Pediatr Res* 2006;60:435–39
10. Mukherjee P, McKinstry RC. **Diffusion tensor imaging and tractography of human brain development**. *Neuroimaging Clin N Am* 2006;16:19–43, vii
11. Huppi PS, Dubois J. **Diffusion tensor imaging of brain development**. *Semin Fetal Neonatal Med* 2006;11:489–97
12. Berman JI, Glass HC, Miller SP, et al. **Quantitative fiber tracking analysis of the optic radiation correlated with visual performance in premature newborns**. *AJNR Am J Neuroradiol* 2009;30:120–24
13. Norcia AM, Tyler CW. **Spatial frequency sweep VEP: visual acuity during the first year of life**. *Vision Res* 1985;25:1399–408
14. Norcia AM, Garcia H, Humphry R, et al. **Anomalous motion VEPs in infants and in infantile esotropia**. *Invest Ophthalmol Vis Sci* 1991;32:436–39
15. Skoczenski AM, Norcia AM. **Development of VEP Vernier acuity and grating acuity in human infants**. *Invest Ophthalmol Vis Sci* 1999;40:2411–17
16. Skoczenski AM, Good WV. **Vernier acuity is selectively affected in infants and children with cortical visual impairment**. *Dev Med Child Neurol* 2004;46:526–32
17. Bassi L, Ricci D, Volzone A, et al. **Probabilistic diffusion tractography of the optic radiations and visual function in preterm infants at term equivalent age**. *Brain* 2008;131:573–82
18. Dumoulin CL, Rohling KW, Piel JE, et al. **Magnetic resonance imaging compatible neonate incubator.** *Concepts in Magnetic Resonance Part B: Magnetic Resonance Engineering* 2002;15:117–28
19. Miller SP, Ferriero DM, Leonard C, et al. **Early brain injury in premature newborns detected with magnetic resonance imaging is associated with adverse early neurodevelopmental outcome**. *J Pediatr* 2005;147:609–16
20. Woods RP, Grafton ST, Holmes CJ, et al. **Automated image registration: I. General methods and intrasubject, intramodality validation**. *J Comput Assist Tomogr* 1998;22:139–52
21. Woods RP, Grafton ST, Watson JD, et al. **Automated image registration: II. Intersubject validation of linear and nonlinear models**. *J Comput Assist Tomogr* 1998;22:153–65
22. Basser PJ, Pierpaoli C. **Microstructural and physiological features of tissues elucidated by quantitative-diffusion-tensor MRI**. *J Magn Reson B* 1996;111:209–19
23. Miller SP, Vigneron DB, Henry RG, et al. **Serial quantitative diffusion tensor MRI of the premature brain: development in newborns with and without injury**. *J Magn Reson Imaging* 2002;16:621–32
24. Norcia AM, Tyler CW, Hamer RD, et al. **Measurement of spatial contrast sensitivity with the swept contrast VEP**. *Vision Res* 1989;29:627–37
25. Odom JV, Bach M, Barber C, et al. **Visual evoked potentials standard (2004)**. *Doc Ophthalmol* 2004;108:115–23
26. Bayley N. *Bayley Scales of Infant and Toddler Development, Third Edition (Bayley-III) Manual.* San Antonio, Texas: PsychCorp (Harcourt Assessment), 2006
27. Zeger SL, Liang KY, Albert PS. **Models for longitudinal data: a generalized estimating equation approach**. *Biometrics* 1988;44:1049–60
28. Beaulieu C. **The basis of anisotropic water diffusion in the nervous system: a technical review**. *NMR Biomed* 2002;15:435–55
29. Song SK, Sun SW, Ju WK, et al. **Diffusion tensor imaging detects and differentiates axon and myelin degeneration in mouse optic nerve after retinal ischemia**. *Neuroimage* 2003;20:1714–22
30. Prayer D, Barkovich AJ, Kirschner DA, et al. **Visualization of nonstructural changes in early white matter development on diffusion-weighted MR images: evidence supporting premyelination anisotropy**. *AJNR Am J Neuroradiol* 2001;22:1572–76
31. Drobyshevsky A, Song SK, Gamkrelidze G, et al. **Developmental changes in diffusion anisotropy coincide with immature oligodendrocyte progression and maturation of compound action potential**. *J Neurosci* 2005;25:5988–97
32. Partridge SC, Mukherjee P, Berman JI, et al. **Tractography-based quantitation of diffusion tensor imaging parameters in white matter tracts of preterm newborns**. *J Magn Reson Imaging* 2005;22:467–74
33. Partridge SC, Mukherjee P, Henry RG, et al. **Diffusion tensor imaging: serial quantitation of white matter tract maturity in premature newborns**. *Neuroimage* 2004;22:1302–14
34. Berman JI, Mukherjee P, Partridge SC, et al. **Quantitative diffusion tensor MRI fiber tractography of sensorimotor white matter development in premature infants**. *Neuroimage* 2005;27:862–71
35. Moskowitz A, Sokol S. **Developmental changes in the human visual system as reflected by the latency of the pattern reversal VEP**. *Electroencephalogr Clin Neurophysiol* 1983;56:1–15
36. Dubois J, Dehaene-Lambertz G, Soares C, et al. **Microstructural correlates of infant functional development: example of the visual pathways**. *J Neurosci* 2008;28:1943–48
37. Counsell SJ, Edwards AD, Chew AT, et al. **Specific relations between neurodevelopmental abilities and white matter microstructure in children born preterm**. *Brain* 2008;131:3201–08
38. Drobyshevsky A, Bregman J, Storey P, et al. **Serial diffusion tensor imaging detects white matter changes that correlate with motor outcome in premature infants**. *Dev Neurosci* 2007;29:289–301
39. Rose J, Mirmiran M, Butler EE, et al. **Neonatal microstructural development of the internal capsule on diffusion tensor imaging correlates with severity of gait and motor deficits**. *Dev Med Child Neurol* 2007;49:745–50
40. Arzoumanian Y, Mirmiran M, Barnes PD, et al. **Diffusion tensor brain imaging findings at term-equivalent age may predict neurologic abnormalities in low birth weight preterm infants**. *AJNR Am J Neuroradiol* 2003;24:1646–53
41. Krishnan ML, Dyet LE, Boardman JP, et al. **Relationship between white matter apparent diffusion coefficients in preterm infants at term-equivalent age and developmental outcome at 2 years**. *Pediatrics* 2007;120:e604–09